Int. J. Electrochem. Sci., 8 **(2013)** 5067 - 5085

International Journal of
ELECTROCHEMICAL
SCIENCE
www.electrochemsci.org

Ionic Conductivity and Thermophysical Properties of 1-Butyl-1-Methylpyrrolidinium Butyl Sulfate and its Binary Mixtures with Poly(ethylene glycol) at Various Temperatures

Tzi-Yi Wu[*], *Lin Hao, Pin-Rong Chen, Jian-Wei Liao*

Department of Chemical and Materials Engineering, National Yunlin University of Science and Technology, Yunlin 64002, Taiwan, ROC
[*]E-mail: wuty@yuntech.edu.tw

Received: 18 February 2013 / *Accepted:* 16 March 2013 / *Published:* 1 April 2013

The work studies the synthesis and thermophysical characterization of butylsulfate-based Ionic Liquid (IL) [PyrMB][$BuSO_4$]. The synthesized IL is characterized by NMR spectroscopy, elemental analysis, and Karl Fischer titration. Thermophysical properties such as density, ρ, viscosity, η, and conductivity, κ, for the binary mixture of butylsulfate-based IL [PyrMB][$BuSO_4$] with poly(ethylene glycol) (PEG) [M_w = 200] are measured over the whole composition range. The thermal expansion coefficient of neat [PyrMB][$BuSO_4$] and its binary mixtures is ascertained using the experimental density results, and their excess volume expansivity is also estimated. The temperature dependence of viscosity and conductivity over the whole composition range can be described by the Vogel−Tammann−Fulcher (VTF) equation, and the maximum of conductivity is located at x_{PEG200} = 0.59 and corresponds to a value of 1.71 mS cm^{-1} at 333.15 K. The excess properties and deviations are fitted to the Redlich−Kister polynomial equation to obtain the binary coefficients and the standard errors. The variation of these properties with composition of the binary mixtures is discussed in terms of molecular interactions between components and structural effects.

Keywords: ionic liquids, binary mixture, viscosity, conductivity, Vogel-Tammann-Fulcher equation, excess properties, deviations

1. INTRODUCTION

Room temperature ionic liquids (ILs) are typically salts that contain at least one organic cation or anion and have melting points below or not far above ambient temperatures [1]. The physicochemical properties of ILs can be molecularly designed to positively affect different kinds of processes by varying these anions and cations [2-5]. During the past decade, ionic liquids (ILs) have attracted increasing attention and intensive investigation and witnessed a steady growth from the

academics to industry due to their distinctive properties, such as wide temperature range of application, high thermal stability [3-5], nonflammability, wide electrochemical window [6-9], and high electrical conductivity [10-13]. They have been used in a broad variety of synthesis [14,15], corrosion inhibition [16-20], biotechnology [21-24], and nano technology [25-32], especially as promising "green" electrolyte for electrochemical devices such as dye-sensitized solar cells [33–38], lithium ion batteries [39-42], sensors [43-55], and fuel cells [56], but experimental data of physicochemical properties [57-61] are still scarce. Alkylsulfate-based ILs are some of the most promising ILs to be applied in academic investigations and industrial processes, since most of these ILs can be easily synthesized at a reasonable cost [62]. So far the viscosity of sulfate-based ILs are 1 to 3 orders of magnitude greater than those of traditional organic liquids, which affect the rate of mass transfer, leading to much more power needed for mixing in liquid reactions or separation processes. In some current studies, the problem of high viscosity can be resolved partially by means of adding organic solvents to pure ionic liquid [63]. Although the addition of organic solvents into ILs decreases the viscosity of mixture significantly, the conventional organic solvents has high volatility due to their boiling temperature are below 80 ^{o}C. Accordingly, some scientists studied the thermodynamic properties of ethylene glycol derivatives instead of conventional organic solvents. Poly(ethylene glycol) (PEG) is one of the ethylene glycol derivatives, PEG of various molecular weights have been widely used in processes across many industrial sectors, as a result of being non-toxic, biodegradable, inexpensive, widely available, and with a very low volatility [64,65]. Low molecular weight PEG (M_w = 200) is liquid at room temperature, making it easy to combine with ILs, generate solvent systems, and thus use in advanced, environmentally friendly processes [65].

In the present research, the density, viscosity, and conductivity of a sulfate-based IL ([PyrMB][$BuSO_4$]) and its binary mixture with PEG200 over the whole composition range and temperatures between (293.15 and 353.15) K at atmospheric pressure are estimated. From these experimental results, excess molar volume, excess volume expansivity, and viscosity deviations from the ideal behavior were characterized. The excess properties were calculated and then correlated, at each temperature, as a function of composition by a Redlich-Kister-type equation. The impact nature of the solute on the ionic conductivity and thermophysical properties of binary mixture was investigated in detail.

2. EXPERIMENTAL

2.1. Materials

Poly(ethylene glycol)s, dibutyl sulfate, and 1-methylpyrrolidine were obtained from commercial suppliers and used without further purification. The poly(ethylene glycol)s of average molar mass 200 was purchased from Showa Chemical Industry Co., Ltd, Japan, dibutyl sulfate (95 %) and 1-methylpyrrolidine (>98 %) was purchased from Tokyo Chemical Industry Co., Ltd.

2.2. 1-Butyl-1-methylpyrrolidinium butyl sulfate ([PyrMB][BuSO$_4$])

Dibutyl sulfate (75.7 g, 360 mmol) was added dropwise to a solution of equal molar amounts of 1-methylpyrrolidine (30.65 g, 360 mmol) in 200 mL toluene, and then cooled in an ice-bath under nitrogen at a rate that maintained the reaction temperature below 313.15 K (highly exothermic reaction). The reaction mixture was stirred at room temperature for 4h. After the reaction stopped, the upper organic phase of the resulting mixture was decanted, and the lower ionic liquid phase was washed with ethyl acetate (4 x 70 mL). After the last washing, the remaining ethyl acetate was removed by rotavapor under reduced pressure. The IL obtained was dried by heating at (343.15 to 353.15) K and stirring under a high vacuum (2×10^{-1} Pa) for 48 h. In order to reduce the water content to negligible values (lower than 0.03 mass %), a vacuum (2×10^{-1} Pa) and moderate temperature (343.15 K) were applied to the IL for 2 days. The IL was kept in bottles under an inert gas. The structure of [PyrMB][BuSO$_4$] is shown in Figure 1.

Yield: 91 %. ^{1}H NMR (300 MHz, D_2O, ppm): 3.95 (t, 2H, -C$\underline{H}_2$SO$_4$), 3.38 (m, 4H, N-C$\underline{H}_2$-), 3.21 (m, 2H, N-C$\underline{H}_2$-), 2.92 (s, 3H, N-C$\underline{H}_3$), 2.10 (m, 4H, N-CH$_2$C$\underline{H}_2$-), 1.67 (m, 2H, -C$\underline{H}_2$CH$_2$SO$_4$), 1.55 (m, 2H, N-CH$_2$C$\underline{H}_2$-), 1.28 (m, 4H, N-CH$_2$CH$_2$C$\underline{H}_2$- and -C$\underline{H}_2$CH$_2$CH$_2$SO$_4$), 0.82 (m, 6H, N-CH$_2$CH$_2$CH$_2$C$\underline{H}_3$ and C$\underline{H}_3$CH$_2$CH$_2$CH$_2$SO$_4$). Elem. Anal. Calcd. for $C_{13}H_{29}NO_4S$: C, 52.85 %; H, 9.89 %; N, 4.74 %. Found: C, 52.68 %; H, 9.79 %; N, 4.65 %.

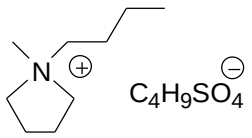

Figure 1. Molecular structure of 1-butyl-1-methylpyrrolidinium butyl sulfate ([PyrMB][BuSO$_4$]).

2.3. Measurements

The conductivity (κ) of the ionic liquids was systematically measured with a conductivity meter (LF 340, WTW, Germany) and a standard conductivity cell (TetraCon 325, WTW, Germany). The cell constant was determined by calibration after each sample measurement using an aqueous 0.01 M KCl solution. The density of the ILs was measured with a dilatometer, which was calibrated by measuring the density of neat glycerin at 30, 40, 50, 60, 70, and 80 ^{o}C. The dilatometer was placed in a thermostatic water bath (TV-4000, TAMSON) whose temperature was regulated to within ± 0.01 K. To measure density, IL or a binary mixture was placed into the dilatometer up to the mark, the top of the capillary tube (located on the top of the dilatometer) was sealed, and the dilatometer (with capillary tube) was placed into a temperature bath for 10 min to allow the temperature to equilibrate. The main interval between the two marks in the capillary tube was 0.01 cm^3, and the minor interval between two marks was 0.001 cm^3. From the correction coefficient of glycerin in capillary tube at various temperatures, we can calculate the density of neat IL or binary system by the expanded volume of liquid in the capillary tube at various temperatures. Each sample was measured at least three times to determine an average value, and the values of the density were ±0.0001 g/mL. The viscosity (η) of the

IL was measured using a calibrated modified Ostwald viscometer (Cannon-Fenske glass capillary viscometers, CFRU, 9721-A50). The viscometer capillary diameter was 1.2 mm, as measured using a caliper (model No. PD-153) with an accuracy of ± 0.02 mm. The viscometer was placed in a thermostatic water bath (TV-4000, TAMSON) whose temperature was regulated to within ± 0.01 K. The flow time was measured using a stopwatch with a resolution of 0.01 s. For each IL, the experimental viscosity was obtained by averaging three to five flow time measurements. The water content of synthesized IL [PyrMB][$BuSO_4$] was determined using the Karl–Fischer method; the content was below 300 ppm. The nuclear magnetic resonance (NMR) spectra of the synthesized IL were recorded on a BRUKER AV300 spectrometer and calibrated with tetramethylsilane (TMS) as the internal reference.

3. RESULTS AND DISCUSSION

3.1. Density and excess molar volume

The densities of neat IL [PyrMB][$BuSO_4$], neat PEG200, and {PEG200 (1) + [PyrMB][$BuSO_4$] (2)} binary mixture over the temperature range (293.15 to 353.15) K and at atmospheric pressure are presented in Table 1 and Figure 2. As shown in Figure 2, the trend of density for the binary system with respect to temperature was decreased with increasing temperature. The variations of the densities with concentration at the different temperatures studied are shown in Figure 3, from analysis of the data, it was found that the densities depend more strongly on the mole fraction of PEG200 in the mixture than on temperature.

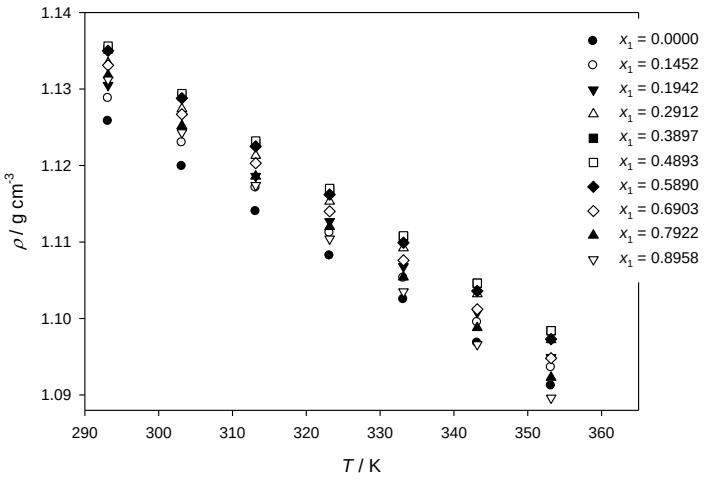

Figure 2. ρ vs. T plot of the {PEG200 (1) + [PyrMB][$BuSO_4$] (2)} binary system.

A third-order polynomial was found to satisfactorily correlate the change of density with various compositions:

$$\rho = a_0 + a_1 \cdot x_1 + a_2 \cdot x_1^2 + a_3 \cdot x_1^3 \quad (1)$$

where x_1 is the mole fractions of PEG200 and a_0, a_1, a_2, and a_3 refer to the fit coefficients. Fit parameters are listed in Table 2 for the mixtures.

Table 1. Experimental density (ρ) and excess molar volume (V_m^E) for the binary system {PEG200 (1) + [PyrMB][$BuSO_4$] (2)}

x_1	*T*/K												
	293.15	298.15	303.15	308.15	313.15	318.15	323.15	328.15	333.15	338.15	343.15	348.15	353.15
	ρ/g ·cm^{-3}												
0	1.1258	1.1228	1.1199	1.1169	1.1140	1.1111	1.1082	1.1053	1.1025	1.0996	1.0968	1.0940	1.0912
0.1452	1.1288	1.1259	1.1230	1.1200	1.1171	1.1142	1.1112	1.1083	1.1053	1.1024	1.0995	1.0965	1.0936
0.1942	1.1305	1.1275	1.1245	1.1216	1.1186	1.1157	1.1127	1.1097	1.1068	1.1038	1.1008	1.0979	1.0949
0.2912	1.1334	1.1304	1.1274	1.1243	1.1213	1.1183	1.1153	1.1123	1.1092	1.1062	1.1032	1.1002	1.0972
0.3897	1.1352	1.1321	1.1291	1.1260	1.1229	1.1199	1.1168	1.1138	1.1107	1.1076	1.1046	1.1015	1.0984
0.4893	1.1356	1.1325	1.1294	1.1263	1.1232	1.1201	1.1170	1.1139	1.1108	1.1077	1.1046	1.1015	1.0984
0.5890	1.1350	1.1319	1.1288	1.1256	1.1225	1.1193	1.1162	1.1131	1.1099	1.1068	1.1036	1.1005	1.0973
0.6903	1.1331	1.1299	1.1267	1.1235	1.1203	1.1172	1.1140	1.1108	1.1076	1.1044	1.1012	1.0980	1.0948
0.7922	1.1318	1.1285	1.1252	1.1219	1.1186	1.1153	1.1120	1.1087	1.1054	1.1021	1.0988	1.0956	1.0923
0.8958	1.1312	1.1278	1.1243	1.1208	1.1174	1.1139	1.1104	1.1070	1.1035	1.1000	1.0966	1.0931	1.0896
1	1.1312	1.1273	1.1234	1.1195	1.1157	1.1119	1.1081	1.1044	1.1007	1.0970	1.0933	1.0896	1.0860
	V_m^E/cm^3 mol^{-1}												
0	0.0000	0.0000	0.0000	0.0000	0.0000	0.0000	0.0000	0.0000	0.0000	0.0000	0.0000	0.0000	0.0000
0.1452	-0.5572	-0.5884	-0.6161	-0.6404	-0.6613	-0.6787	-0.6925	-0.7028	-0.7096	-0.7127	-0.7123	-0.7081	-0.7003
0.1942	-0.8575	-0.8917	-0.9225	-0.9498	-0.9737	-0.9942	-1.0111	-1.0245	-1.0343	-1.0406	-1.0432	-1.0422	-1.0375
0.2912	-1.3539	-1.3931	-1.4289	-1.4614	-1.4903	-1.5159	-1.5379	-1.5564	-1.5714	-1.5828	-1.5906	-1.5947	-1.5952
0.3897	-1.5730	-1.6197	-1.6630	-1.7029	-1.7394	-1.7726	-1.8022	-1.8284	-1.8511	-1.8702	-1.8858	-1.8978	-1.9061
0.4893	-1.4983	-1.5521	-1.6026	-1.6498	-1.6936	-1.7341	-1.7711	-1.8047	-1.8348	-1.8615	-1.8846	-1.9041	-1.9201
0.5890	-1.2361	-1.2970	-1.3547	-1.4090	-1.4601	-1.5078	-1.5522	-1.5931	-1.6306	-1.6647	-1.6953	-1.7224	-1.7459
0.6903	-0.7359	-0.8013	-0.8634	-0.9222	-0.9777	-1.0300	-1.0788	-1.1243	-1.1663	-1.2049	-1.2400	-1.2717	-1.2997
0.7922	-0.3606	-0.4235	-0.4831	-0.5394	-0.5923	-0.6418	-0.6878	-0.7304	-0.7695	-0.8051	-0.8371	-0.8655	-0.8903
0.8958	-0.1410	-0.1915	-0.2384	-0.2818	-0.3216	-0.3578	-0.3903	-0.4192	-0.4443	-0.4656	-0.4832	-0.4969	-0.5068
1	0.0000	0.0000	0.0000	0.0000	0.0000	0.0000	0.0000	0.0000	0.0000	0.0000	0.0000	0.0000	0.0000

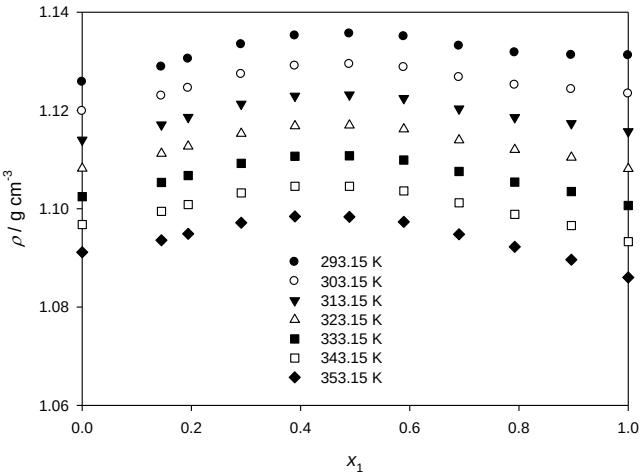

Figure 3. ρ of the {PEG200 (1) + [PyrMB][$BuSO_4$] (2)} binary system as a function of concentration at various temperatures.

The correlation constants for Eq. (1) were established using the least square method and are presented in Table 2 along with the standard deviation estimated using the following equation:

$$\sigma = [\frac{\Sigma(Z_{exp} - Z_{cal})^2}{n}]^{1/2} \quad (2)$$

where n is the number of experimental points, and Z_{exp} and Z_{cal} are the experimental and calculated values, respectively.

Table 2. Coefficients of polynomial[a] for the correlation of the density, (ρ/g·cm^{-3}) in function of concentration at different temperatures of the binary systems {PEG200 (1) + [PyrMB][BuSO$_4$] (2)}

T/K	a_0 / g cm^{-3}	a_1 / g cm^{-3}	a_2 / g cm^{-3}	a_3 / g cm^{-3}	σ
293.15	1.1248	0.0455	-0.0638	0.024	0.000840
298.15	1.1219	0.0447	-0.0617	0.0217	0.000800
303.15	1.119	0.0439	-0.0596	0.0195	0.000764
308.15	1.1161	0.0431	-0.0575	0.0173	0.000732
313.15	1.1132	0.0422	-0.0554	0.0152	0.000704
318.15	1.1103	0.0413	-0.0533	0.0132	0.000680
323.15	1.1075	0.0403	-0.0512	0.0112	0.000660
328.15	1.1046	0.0393	-0.0492	0.0093	0.000640
333.15	1.1018	0.0382	-0.0471	0.0074	0.000625
338.15	1.0989	0.0372	-0.045	0.0055	0.000613
343.15	1.0961	0.036	-0.043	0.0037	0.000606
348.15	1.0933	0.0349	-0.0409	0.002	0.000596
353.15	1.0905	0.0337	-0.0389	0.0003	0.000592

[a] $\rho = a_0 + a_1 \cdot x_1 + a_2 \cdot x_1^2 + a_3 \cdot x_1^3$

As can be seen from the Table 1, the value of the density decreases with increasing temperature eventhough the variation is very small. If the variation of the density with the temperature is considered as linear, then the change in the calculated thermal expansion coefficient values becomes nearly constant. In order to have an improved accuracy, a second order polynomial of the eqn. (3) was used to correlate the variation of the density with the temperature for {PEG200 (1) + [PyrMB][BuSO$_4$] (2)} binary system.

$$\rho = b_0 + b_1 \cdot T + b_2 \cdot T^2 \qquad (3)$$

where T is the temperature and b_0, b_1, and b_2 are the correlation coefficients. The correlation coefficients are listed in Table 3 together with the standard deviations (σ) calculated using Eq. (2).

Excess thermodynamic properties are of great importance for understanding the nature of molecular interaction in binary mixtures. The excess molar volume, V_m^E, which is the difference between the real and ideal mixing behaviors, is defined by:

$$V_m^E = V_m - x_1 V_1^o - x_2 V_2^o \qquad (4)$$

where V_m represents the volume of a mixture containing one mole of (PEG200 + [PyrMB][BuSO$_4$]), x_1 and x_2 are the mole fractions of components 1 (PEG200) and 2 ([PyrMB][BuSO$_4$]), respectively, and V_1^0 and V_2^0 are the molar volumes of the pure components. The

excess molar volumes of mixtures over the entire composition range were calculated from our measurements of density according to the following equation:

Table 3. The adjustable parameters of density ($\rho = b_0 + b_1 \cdot T + b_2 \cdot T^2$) at various temperature for neat PEG200 ($x_1 = 1$), [PyrMB][$BuSO_4$] ($x_1 = 0$), and binary system {PEG200 (1) + [PyrMB][$BuSO_4$] (2)}.

x_1	b_0	b_1	b_2	σ
0	1.326	-0.00077105	0.0000003	0.00003
0.1452	1.301	-0.000588	0	0.00023
0.1942	1.304	-0.000593	0	0.00032
0.2912	1.31	-0.000604	0	0.00047
0.3897	1.315	-0.000613	0	0.00009
0.4893	1.318	-0.000621	0	0.00034
0.5890	1.319	-0.000629	0	0.00045
0.6903	1.32	-0.000639	0	0.00046
0.7922	1.325	-0.000658	0	0.00036
0.8958	1.335	-0.000694	0	0.00030
1	1.405	-0.00108	0.00000051	0.00112

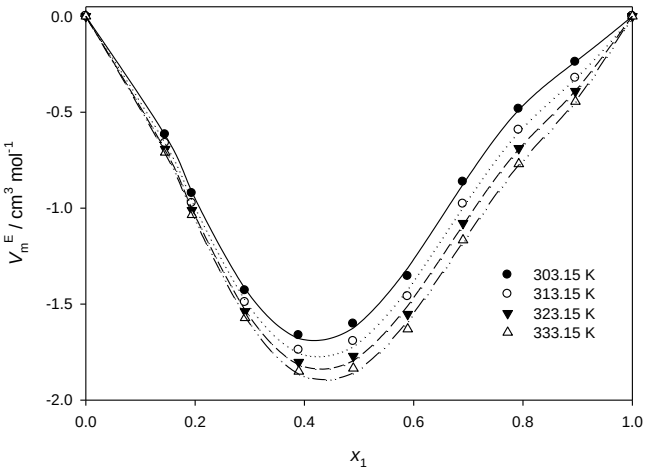

Figure 4. Excess molar volumes for the binary system {PEG200 (1) + [PyrMB][$BuSO_4$] (2)} and fitted curves using the Redlich-Kister parameters.

$$V_m^E = \frac{x_1 M_1 + x_2 M_2}{\rho} - \frac{x_1 M_1}{\rho_1} - \frac{x_2 M_2}{\rho_2} \quad (5)$$

where ρ_1, ρ_2, and ρ are the densities of neat PEG200, [PyrMB][$BuSO_4$], and their mixture, respectively; M_1 and M_2 are the molar masses of PEG200 and [PyrMB][$BuSO_4$], respectively. The V_m^E values of mixtures are summarized in Table 1. The excess molar volumes of mixtures versus the mole

fraction of PEG200 from 293.15 to 353.15 K are plotted in Figure 4. The excess molar volume of the binary system is mainly concerned with the weak chemical interactions, the physical and structural characteristics of the system components. If the chemical or nonchemical interaction of the same components is the dominant way of the interaction, the excess volume of the mixture should be positive. If the molecules of the components have a more effective packing in the mixture than that in the pure component, that is, the attracting interaction between the molecules of two components is the dominant way, the excess molar volume of the binary system should be negative [66]. As shown in Figure 4, the excess molar volumes are asymmetric and negative for all of the systems studied over the entire composition range, the minimum of V_m^E is reached at a mole fraction of PEG200 near $x_1 = 0.4$, and the absolute values of the excess volume increase with increasing temperature. The molar volume for [PyrMB][$BuSO_4$] is 262.43 cm^3 mol^{-1} at T = 293.15 K, which is greater than the molar volumes of PEG200 (176.81 cm^3 mol^{-1}) at T = 293.15 K. The large difference between molar volumes of the molecular liquid and [PyrMB][$BuSO_4$] indicates that it is possible that the relatively small organic molecules fit into the interstices upon mixing. Therefore, the filling effect of organic molecular liquids in the interstices of ionic liquids, and the ion–dipole interactions between poly(ethylene glycol) oligomer and the butylsulfate-based ionic liquids, all contribute to the negative values of the molar excess volumes.

3.2. Volume expansivity and excess volume expansivity

Density results for the PEG200 and [PyrMB][$BuSO_4$] binary system studied in current work were also used to derive the coefficient of thermal expansion. From the relationship of ρ vs. T, the volume expansivity (coefficient of thermal expansion), α, is defined as:

$$\alpha = \frac{1}{V}\left(\frac{\partial V}{\partial T}\right)_p = -\frac{1}{\rho}\left(\frac{\partial \rho}{\partial T}\right)_p \qquad (6)$$

where subscript p indicates constant pressure. The α values of pure [PyrMB][$BuSO_4$] and PEG200, and their mixture are summarized in Table 4. The values indicate that the thermal expansion coefficient of this binary mixture (PEG200 + [PyrMB][$BuSO_4$]) increases with increasing temperature and increases with increasing mole fraction of the PEG200.

The corresponding excess function α^E (excess volume expansivity) was calculated using:

$$\alpha^E = \alpha - \varphi_1^{id}\alpha_1 - \varphi_2^{id}\alpha_2 \qquad (7)$$

where φ_1^{id} is an ideal volume fraction given by the following relation:

$$\varphi_1^{id} = \frac{x_1 V_{m1}}{x_1 V_{m1} + x_2 V_{m2}} \qquad (8)$$

where V_{mi} is the molar volume of pure component *i*.

Table 4. Experimental volume expansivity (α) and the excess volume expansivity (α^E) for the binary system {PEG200 (1) + [PyrMB][$BuSO_4$] (2)}

x_1	T/K												
	293.15	298.15	303.15	308.15	313.15	318.15	323.15	328.15	333.15	338.15	343.15	348.15	353.15
	$10^4\,\alpha/K^{-1}$												
0	5.1245	5.1380	5.1516	5.1651	5.1787	5.1922	5.2058	5.2193	5.2329	5.2464	5.2600	5.2735	5.2871
0.1452	5.2053	5.2189	5.2325	5.2462	5.2600	5.2739	5.2878	5.3018	5.3159	5.3300	5.3443	5.3586	5.3730
0.1942	5.2438	5.2576	5.2715	5.2854	5.2994	5.3135	5.3276	5.3418	5.3561	5.3705	5.3850	5.3995	5.4141
0.2912	5.3299	5.3443	5.3586	5.3731	5.3877	5.4023	5.4170	5.4318	5.4466	5.4616	5.4766	5.4917	5.5069
0.3897	5.3973	5.4120	5.4268	5.4417	5.4567	5.4717	5.4869	5.5021	5.5174	5.5328	5.5483	5.5638	5.5795
0.4893	5.4667	5.4818	5.4971	5.5124	5.5278	5.5433	5.5589	5.5745	5.5903	5.6061	5.6221	5.6381	5.6542
0.5890	5.5372	5.5527	5.5683	5.5840	5.5998	5.6157	5.6317	5.6477	5.6639	5.6801	5.6965	5.7129	5.7294
0.6903	5.6358	5.6517	5.6677	5.6838	5.7000	5.7163	5.7327	5.7492	5.7657	5.7824	5.7992	5.8160	5.8330
0.7922	5.8175	5.8344	5.8515	5.8687	5.8860	5.9033	5.9208	5.9384	5.9561	5.9739	5.9918	6.0098	6.0279
0.8958	6.1313	6.1502	6.1691	6.1882	6.2074	6.2268	6.2462	6.2658	6.2855	6.3053	6.3252	6.3453	6.3655
1	6.6532	6.6763	6.6993	6.7224	6.7455	6.7685	6.7916	6.8146	6.8377	6.8607	6.8838	6.9069	6.9299
	$10^4\,\alpha^E/K^{-1}$												
0	0.0000	0.0000	0.0000	0.0000	0.0000	0.0000	0.0000	0.0000	0.0000	0.0000	0.0000	0.0000	0.0000
0.1452	-0.0762	-0.0772	-0.0782	-0.0792	-0.0800	-0.0808	-0.0815	-0.0822	-0.0827	-0.0832	-0.0837	-0.0840	-0.0843
0.1942	-0.0942	-0.0954	-0.0966	-0.0977	-0.0987	-0.0997	-0.1006	-0.1014	-0.1021	-0.1028	-0.1033	-0.1038	-0.1043
0.2912	-0.1259	-0.1275	-0.1289	-0.1302	-0.1315	-0.1327	-0.1339	-0.1349	-0.1359	-0.1368	-0.1376	-0.1383	-0.1389
0.3897	-0.1870	-0.1889	-0.1908	-0.1926	-0.1943	-0.1959	-0.1975	-0.1989	-0.2003	-0.2016	-0.2028	-0.2040	-0.2050
0.4893	-0.2576	-0.2600	-0.2623	-0.2646	-0.2668	-0.2689	-0.2709	-0.2728	-0.2746	-0.2764	-0.2780	-0.2796	-0.2811
0.5890	-0.3382	-0.3412	-0.3441	-0.3470	-0.3497	-0.3524	-0.3550	-0.3574	-0.3598	-0.3621	-0.3644	-0.3665	-0.3685
0.6903	-0.4064	-0.4100	-0.4136	-0.4170	-0.4204	-0.4236	-0.4268	-0.4299	-0.4329	-0.4358	-0.4386	-0.4413	-0.4439
0.7922	-0.4073	-0.4110	-0.4146	-0.4181	-0.4214	-0.4247	-0.4279	-0.4310	-0.4339	-0.4368	-0.4396	-0.4422	-0.4448
0.8958	-0.2968	-0.2998	-0.3026	-0.3053	-0.3079	-0.3104	-0.3128	-0.3151	-0.3172	-0.3192	-0.3211	-0.3228	-0.3245
1	0.0000	0.0000	0.0000	0.0000	0.0000	0.0000	0.0000	0.0000	0.0000	0.0000	0.0000	0.0000	0.0000

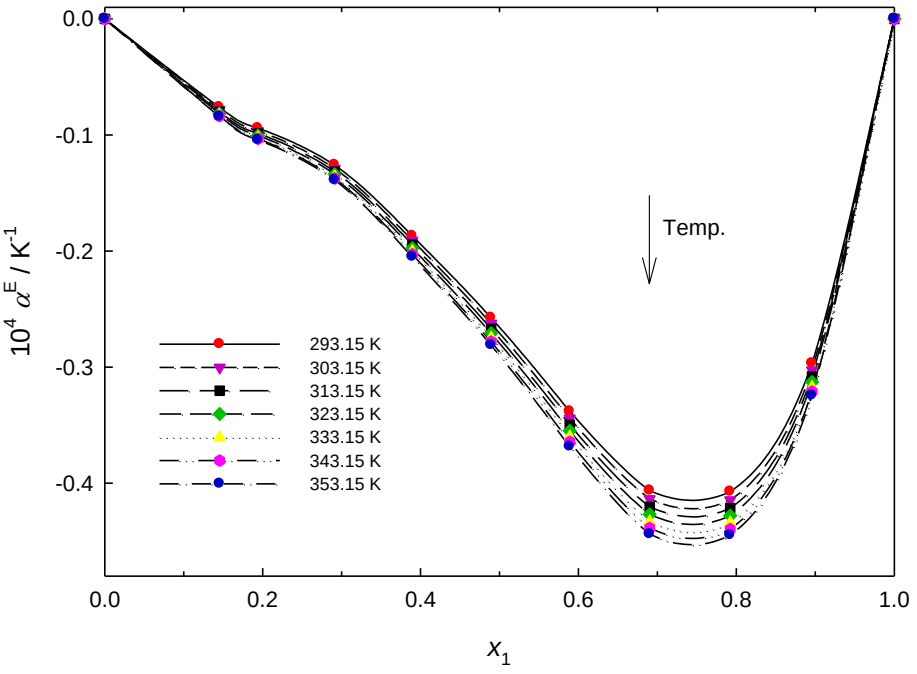

Figure 5. Plot of excess volume expansivity, α^E, of the {PEG200 (1) + [PyrMB][$BuSO_4$] (2)} binary system versus mole fraction x_1 at various temperatures.

Typical concentration dependencies of excess volume expansivity are given in Figure 5 for the {PEG200 + [PyrMB][$BuSO_4$]} binary system. The values of excess thermal coefficient α^E are found to

be negative over the whole composition range for the binary system at 293.15 ~ 353.15 K. The curves are asymmetrical, with the minimum located at the IL mole fraction of about 0.8. In general, negative α^E values indicate the presence of strong interaction between the components in the mixtures [67]. The trends observed in α^E values for the present mixtures suggest the formation of H-bonding between unlike molecules which is stronger in {PEG200 + [PyrMB][$BuSO_4$]} binary system. The increasing negative α^E values for {PEG200 + [PyrMB][$BuSO_4$]} with increase in temperature indicate enhanced unlike interaction between components of the mixture, that is, more destruction of order during mixing contributes negatively to α^E.

3.3. Viscosity

Since ILs are more viscous than conventional solvents, in most applications, they can be used in mixtures with other less viscous compounds. Therefore, the viscosity of pure ILs and their mixtures with PEG oligomer (or conventional solvents) is an important property and their knowledge is primordial for each industrial processes [68,69]. The measured dynamic viscosities, η, for the neat PEG200, neat [PyrMB][$BuSO_4$], and {PEG200 + [PyrMB][$BuSO_4$]} binary mixture as a function of temperature over the whole composition range are shown in Figure 6 and their data are listed in Table 5, the viscosities of the mixtures decrease rapidly when PEG oligomer are added to the ionic liquid, especially at lower temperatures. The fitting lines in Figure 6 were calculated with the following fourth-order polynomial equation:

$$\eta = c_0 + c_1 \cdot x_1 + c_2 \cdot x_1^2 + c_3 \cdot x_1^3 + c_4 \cdot x_1^4 \qquad (9)$$

where x_1 is the mole fractions of PEG200 and c_0, c_1, c_2, c_3, and c_4 refer to the fit coefficients. The parameters of correlation are shown in Table 6.

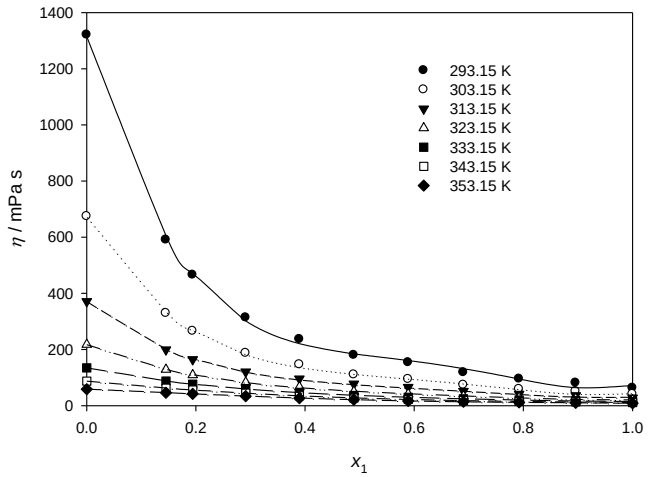

Figure 6. Dynamic viscosity, η, for the {PEG200 (1) + [PyrMB][$BuSO_4$] (2)} binary system as a function of mole fractions of the PEG200 at different temperatures. Lines represent the polynomial correlation.

Table 5. Experimental dynamic viscosity (η) and viscosity deviation ($\Delta\eta$) for the binary system {PEG200 (1) + [PyrMB][$BuSO_4$] (2)}

x_1	*T*/K												
	293.15	298.15	303.15	308.15	313.15	318.15	323.15	328.15	333.15	338.15	343.15	348.15	353.15
	η/mPa·s												
0	1320.9	934.3	674.5	496.1	371.2	282.1	217.6	170.0	134.5	107.7	87.1	71.2	58.7
0.1452	590.7	436.2	329.4	253.9	199.2	158.9	128.6	105.5	87.6	73.5	62.3	53.3	46.0
0.1942	465.6	347.5	265.6	207.2	164.7	133.1	109.1	90.7	76.3	64.9	55.7	48.3	42.2
0.2912	313.4	239.5	187.0	148.9	120.5	99.1	82.6	69.7	59.4	51.2	44.5	39.0	34.5
0.3897	236.7	184.6	146.3	117.7	95.9	79.2	66.0	55.7	47.4	40.6	35.1	30.6	26.9
0.4893	179.9	139.6	110.4	88.7	72.3	59.8	50.1	42.4	36.2	31.2	27.2	23.8	21.0
0.5890	154.0	119.4	94.1	75.3	61.1	50.2	41.8	35.1	29.8	25.5	22.0	19.1	16.7
0.6903	118.5	92.6	73.6	59.4	48.5	40.2	33.6	28.4	24.2	20.9	18.1	15.8	13.9
0.7922	95.4	74.2	58.9	47.5	38.9	32.3	27.1	23.1	19.8	17.2	15.0	13.2	11.7
0.8958	81.1	63.9	51.2	41.5	34.2	28.5	24.0	20.4	17.5	15.1	13.2	11.6	10.2
1	62.9	50.5	41.0	33.7	28.0	23.5	19.9	17.0	14.6	12.6	11.0	9.7	8.5
	$\Delta\eta$/mPa·s												
0	0.0	0.0	0.0	0.0	0.0	0.0	0.0	0.0	0.0	0.0	0.0	0.0	0.0
0.1452	-547.5	-369.8	-253.0	-175.1	-122.1	-85.7	-60.2	-42.3	-29.5	-20.4	-13.7	-8.9	-5.4
0.1942	-611.1	-415.2	-285.9	-199.1	-139.8	-98.8	-70.0	-49.6	-34.7	-24.4	-16.6	-11.0	-6.8
0.2912	-641.1	-437.4	-303.0	-212.6	-150.7	-107.7	-77.4	-55.8	-39.1	-28.8	-20.4	-14.2	-10.3
0.3897	-594.0	-405.3	-281.3	-198.2	-141.5	-102.2	-74.5	-54.7	-40.5	-30.0	-22.3	-16.6	-12.3
0.4893	-525.4	-362.2	-254.1	-181.1	-125.5	-95.7	-70.8	-52.8	-39.6	-29.9	-22.7	-17.3	-13.1
0.5890	-426.0	-294.4	-207.3	-148.4	-103.4	-79.6	-59.4	-44.8	-34.1	-26.2	-20.3	-15.8	-12.4
0.6903	-334.0	-231.6	-163.6	-117.6	-82.6	-63.4	-47.5	-36.0	-27.5	-21.2	-16.5	-12.9	-10.1
0.7922	-228.9	-159.9	-113.8	-82.3	-57.9	-44.9	-32.0	-25.7	-19.7	-15.2	-11.8	-9.2	-7.2
0.8958	-112.9	-78.7	-55.9	-40.4	-27.7	-22.0	-15.2	-12.6	-9.6	-7.4	-5.8	-4.5	-3.5
1	0.0	0.0	0.0	0.0	0.0	0.0	0.0	0.0	0.0	0.0	0.0	0.0	0.0

Table 6. Coefficients of polynomial[a] for the correlation of the viscosity, (η / mPa s) in function of concentration at different temperatures of the binary systems {PEG200 (1) + [PyrMB][$BuSO_4$] (2)}

T/K	c_0 / mPa s	c_1 / mPa s	c_2 / mPa s	c_3 / mPa s	C_4 / mPa s	σ
293.15	1315.4	-6870.1	15960	-16688	6354.3	10.75
298.15	930.69	-4670.3	10681	-11113	4226.9	7.27
303.15	672.11	-3218.5	7208.5	-7439.6	2822.2	4.97
308.15	494.54	-2243.1	4888.6	-4986.6	1882.8	3.43
313.15	370.16	-1577.2	3317.5	-3328.1	1247.4	2.38
318.15	281.46	-1116	2240.6	-2194.7	813.22	1.65
323.15	217.13	-792.3	1494.7	-1413	514.09	1.14
328.15	169.75	-562.44	973.49	-870	306.66	0.77
333.15	134.35	-397.53	606.67	-490.8	162.19	0.51
338.15	107.56	-278.12	347.18	-225.19	61.382	0.33
343.15	87.026	-190.98	163.04	-39.091	-8.8892	0.21
348.15	71.108	-126.98	32.285	90.904	-57.63	0.16
353.15	58.636	-79.728	-60.345	181.03	-91.096	0.17

[a] $\eta = c_0 + c_1 \cdot x_1 + c_2 \cdot x_1^2 + c_3 \cdot x_1^3 + c_4 \cdot x_1^4$

The temperature dependence becomes distinctly nonlinear, especially at high [PyrMB][$BuSO_4$] content. The Vogel-Tammann-Fulcher (VTF) equation [70-75] suitably correlates the nonlinear behavior as a function of the temperature, not only the viscosities of the neat IL but also the viscosities of the mixtures for the binary systems through the composition range.

$$\eta = \eta_o \exp[\frac{B}{(T - T_o)}] \quad (10)$$

where η_o, B, and T_o are constants. The parameter T_o is the ideal glass transition temperature, which should be slightly below the experimental glass transition temperature T_g [76]. The adjustable parameters obtained from the VTF correlation were presented in Table 7. The obtained parameters η_o and B change smoothly with composition for binary mixtures.

Table 7. The VTF equation parameters of viscosity ($\eta^{-1} = \eta_o \exp[\frac{-B}{(T - T_o)}]$) and conductivity ($\kappa = \kappa_o \exp[\frac{-B'}{(T - T_o)}]$) for neat PEG200 (x_1 = 1), [PyrMB][$BuSO_4$] (x_1 = 0), and binary system {PEG200 (1) + [PyrMB][$BuSO_4$] (2)}.

x_1	η				κ			
	η_o (mPa s)	T_o (K)	B (K)	R^{2a}	κ_o (mS cm^{-1})	T_o (K)	B' (K)	R^{2a}
0	0.27	181.0	954.0	0.999	79.2	178.8	685.4	0.999
0.1452	0.26	171.2	941.3	0.999	57.7	169.9	626.8	0.999
0.1942	0.43	178.8	797.5	0.999	40.1	179.2	529.7	0.999
0.2912	0.53	179.4	726.4	0.999	52.1	166.2	603.1	0.999
0.3897	0.26	162.9	890.2	0.999	27.4	180.3	438.1	0.999
0.4893	0.23	166.6	845.5	0.999	17.7	195.1	327.2	0.999
0.5890	0.15	164.8	886.5	0.999	21.6	188.3	367.2	0.999
0.6903	0.15	164.7	857.2	0.999	8.8	217.4	200.0	0.999
0.7922	0.17	171.7	770.2	0.999	9.2	202.0	257.8	0.999
0.8958	0.12	164.2	836.0	0.999	4.3	211.0	208.8	0.999
1	0.14	164.9	786.8	0.999	55.6	192.8	981.5	0.999

[a] Correlation coefficient.

The viscosities of the mixtures decrease rapidly when organic oligomers are added to the ionic liquid, this decrease is particularly evident in dilute solutions of organic oligomers in the ionic liquid. The strong coulomb interactions between the $[BuSO_4]^-$ anion and $[PyrMB]^+$ cation are weakened upon mixing with the polar organic oligomers, which leads to a higher mobility of the ions and a lower viscosity of the mixtures [77]. This indicates that the viscosity of ILs could be therefore tuned for several applications by adding an organic solvent or by changing temperature [78].

Due to the wide range of possible molecular interactions between the two components, deviations can occur from ideal behavior. These viscosity deviations can be quantified by the viscosity deviation, $\Delta\eta$, also known as “excess viscosity” in other sources:

$$\Delta\eta/(\text{mPa}\cdot\text{s}) = \eta - x_1\eta_1 - x_2\eta_2 \quad (11)$$

where x_1 and x_2 are the mole fractions of PEG200 and [PyrMB][$BuSO_4$], respectively, and η, η_1, and η_2 are the viscosities (mPa · s) of the solution, the pure solvent, and the pure IL, respectively.
Figure 7 shows the viscosity deviations as a function of the PEG200 mole fraction composition, x_1, and temperature for the {PEG200 + [PyrMB][$BuSO_4$]} binary mixture. The values of viscosity deviations are compared with those obtained from the Redlich–Kister polynomial equation. The viscosity deviation for the mixture show negative deviations from ideality over the whole mole fraction range. Figure 7 also shows that the negative values of viscosity deviations decrease with increasing temperature, this can be attributed to the specific interactions in mixtures, typically hydrogen bonds, break-up as the temperature increases [79]. The minimum value of $\Delta\eta$ is observed at about $x_1 \approx 0.3$, and the viscosity deviation depends on molecular interactions as well as on the size and shape of the molecules [80].

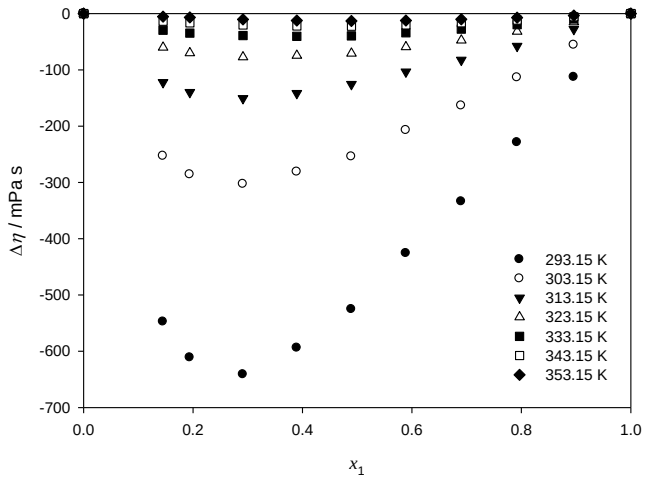

Figure 7. Viscosity deviations, $\Delta\eta$, versus the mole fraction at various temperatures for the binary mixture {PEG200 (1) + [PyrMB][$BuSO_4$] (2)}.

3.4. Conductivity

The experimental data of conductivity of the neat ILs [PyrMB][$BuSO_4$], neat PEG200, and binary system are plotted against the x_1 at various temperatures in Figure 8, together with lines calculated with the four-order polynomial equation:

$$\kappa = d_0 + d_1 \cdot x_1 + d_2 \cdot x_1^2 + d_3 \cdot x_1^3 + d_4 \cdot x_1^4 \qquad (12)$$

where x_1 is the mole fractions of PEG200 and d_0, d_1, d_2, d_3, and d_4 refer to the fit coefficients. The parameters of correlation are shown in Table 8. The conductivities of neat IL [PyrMB][$BuSO_4$], neat PEG200, and binary system at various temperatures were fitted using the VTF equation:

$$\kappa = \kappa_o \exp\left[\frac{-B'}{(T - T_o)}\right] \qquad (13)$$

where T is the absolute temperature and κ_o, B', and T_o are adjustable parameters. The best-fit κ_o (mS cm^{-1}), B' (K), and T_o (K) parameters are given in Table 7. Neat [PyrMB][BuSO$_4$], neat PEG200, and binary system were very well fit by the VTF model over the temperature range studied.

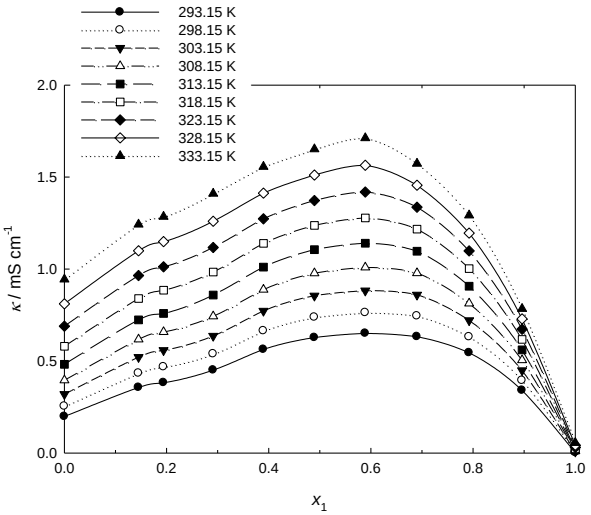

Figure 8. Plot of conductivity, κ, of the {PEG200 (1) + [PyrMB][BuSO$_4$] (2)} binary system versus mole fraction x_1 at various temperatures.

Table 8. Coefficients of polynomial[a] for the correlation of the conductivity, (κ / mS cm^{-1}) in function of concentration at different temperatures of the binary systems {PEG200 (1) + [PyrMB][BuSO$_4$] (2)}

T/K	d_0 / mS cm^{-1}	d_1 / mS cm^{-1}	d_2 / mS cm^{-1}	d_3 / mS cm^{-1}	d_4 / mS cm^{-1}	σ
293.15	0.2019	0.9622	-0.1679	0.734	-1.7284	0.0095
298.15	0.2588	1.1031	-0.2503	0.9086	-2.0181	0.0109
303.15	0.3255	1.2119	-0.1935	0.8565	-2.1971	0.0125
308.15	0.4025	1.3165	-0.1329	0.767	-2.3477	0.0141
313.15	0.4904	1.3712	0.1238	0.3677	-2.3439	0.0156
318.15	0.5894	1.5032	-0.0006	0.4737	-2.5518	0.0171
323.15	0.6999	1.5802	0.0743	0.265	-2.5986	0.0188
328.15	0.8221	1.6427	0.1595	0.0089	-2.6032	0.0208
333.15	0.9562	1.6373	0.4858	-0.6207	-2.4165	0.0233

[a] $\kappa = d_0 + d_1 \cdot x_1 + d_2 \cdot x_1^2 + d_3 \cdot x_1^3 + d_4 \cdot x_1^4$

As shown in Figure 8, it can be seen that the conductivity of the binary mixture increases with increasing amount of PEG200, goes through a maximum, and then goes down to the specific conductivity of the neat PEG200. The conductivity is related to the ion mobility and the number of charge carriers [81]. At a fixed concentration, the ions move faster at higher temperature due to the relatively lower viscosity of the mixture. On the other hand, the composition influences both the ion mobility and the number of charge carriers at a fixed temperature. At the beginning, the number of charge and the ion mobility increase with increasing PEG oligomer composition, the maximum of conductivity is located at x_1 = 0.59 and corresponds to a value of 1.71 mS cm^{-1} at 333.15 K. It can also be observed that the conductivity increases as the temperature increases. The higher temperature may

weaken the influence of aggregation to the conductivity, which suggests that a higher temperature is better for the ILs to act as electrolytes.

Table 9. Redlick–Kister fitting coefficients A_k and the standard deviation σ of the V^E and $\Delta\eta$ for the binary mixture of {PEG200 (1) + [PyrMB][$BuSO_4$] (2)} system.

T/K	A_0	A_1	A_2	A_3	A_4	σ
	V^E/cm^3 mol^{-1}					
293.15	-5.979	-4.906	6.585	5.754	-1.717	0.02687
298.15	-6.200	-4.760	6.464	5.767	-2.022	0.02693
303.15	-6.408	-4.612	6.345	5.774	-2.276	0.02698
308.15	-6.602	-4.461	6.229	5.774	-2.476	0.02701
313.15	-6.782	-4.310	6.116	5.767	-2.623	0.02701
318.15	-6.948	-4.155	6.006	5.753	-2.716	0.02699
323.15	-7.100	-3.999	5.899	5.732	-2.754	0.02692
328.15	-7.239	-3.840	5.795	5.704	-2.738	0.02683
333.15	-7.363	-3.679	5.694	5.669	-2.666	0.02670
338.15	-7.472	-3.515	5.596	5.626	-2.538	0.02654
343.15	-7.568	-3.350	5.501	5.576	-2.353	0.02634
348.15	-7.648	-3.182	5.409	5.518	-2.111	0.02611
353.15	-7.714	-3.011	5.320	5.452	-1.812	0.02586
	$\Delta\eta$/mPa s					
293.15	-2041.4	-1722.6	-1559.2	-955.44	-75.863	3.99496
298.15	-1403.5	-1155.8	-1071.3	-621.92	19.493	3.40180
303.15	-982.61	-784.07	-737.34	-407.09	58.145	2.86725
308.15	-699.22	-535.91	-506.01	-267.6	67.556	2.35258
313.15	-488.76	-395.37	-410.51	-141.18	167.39	0.79245
318.15	-369.17	-251.69	-229.39	-116.46	51.047	1.46189
323.15	-274.15	-172.1	-125.81	-92.603	21.498	1.04339
328.15	-204.41	-117.03	-77.538	-38.334	-8.1478	0.90708
333.15	-153.82	-67.274	-31.134	-47.585	-18.255	0.59539
338.15	-116.64	-44.928	-15.533	-22.312	-0.5591	0.37855
343.15	-89.038	-24.163	6.8654	-15.007	-10.347	0.24263
348.15	-68.279	-9.1813	23.131	-10.367	-18.636	0.17759
353.15	-52.525	-2.4051	26.474	1.5498	-8.5341	0.18640

3.5. Redlich-Kister Equation for Binary System

The binary excess property (V_m^E) and deviations ($\Delta\eta$) at several temperatures were fitted to a Redlich-Kister-type equation [82]:

$$\Delta Y(\text{or } Y^E) = x_1(1-x_1)\sum_{i=0}^{j} A_i(1-2x_1)^i \qquad (14)$$

where ΔY (Y^E) represents V_m^E (cm^3 mol^{-1}) and $\Delta\eta$ (mPa s); x_1 denotes the mole fraction of PEG200, A_i represents the polynomial coefficients, and j is the degree of the polynomial expansion. The correlated results for excess molar volumes (V_m^E), viscosity deviations ($\Delta\eta$), including the values of the fitting parameters A_i together with the standard deviation σ, are given in Table 9, where the tabulated standard deviation σ [83] is defined as:

$$\sigma = [\frac{\Sigma(\Delta Y_{exp} - \Delta Y_{cal})^2}{m-n}]^{1/2} \quad (15)$$

where m is the number of experimental data points and n is the number of estimated parameters. The subscripts "exp" and "cal" denote the values of the experimental and calculated property, respectively. As shown in Table 9, the experimentally derived V_m^E and $\Delta\eta$ values were correlated satisfactorily by the Redlich-Kister equation.

4. CONCLUSIONS

This paper is a systematic characterizations of thermophysical properties for IL binary system. Density, viscosity and conductivity for (PEG200 + [PyrMB][$BuSO_4$]) binary system are presented as a function of temperature at atmospheric pressure, it was demonstrated that viscosity and conductivity were more sensitive to the changes in PEG content or temperature than density, and the viscosity and conductivity of pure IL and (PEG200 + [PyrMB][$BuSO_4$]) binary system at different temperature are fitted using the Vogel–Tammann–Fulcher (VTF) equation with good accuracy. The excess molar volumes, excess volume expansivity, and viscosity deviations show negative deviations from the ideal solution, the results are interpreted in terms of molecular interactions in the (PEG200 + [PyrMB][$BuSO_4$]) binary mixture. The conductivity increases to a maximum value when the concentration of PEG200 is increased and decreases after the maximum, the data obtained will be helpful for the application of the ionic liquids as electrolytes and also useful for the ionic liquids database.

ACKNOWLEDGEMENTS
The authors would like to thank the National Science Council of the Republic of China for financially supporting this project.

References

1. P. Wasserscheid, T. Welton, Ionic Liquids in Synthesis, Second ed. Weinheim, VCH, 2003.
2. T.Y. Wu, I.W. Sun, S.T. Gung, M.W. Lin, B.K. Chen, H.P. Wang, S.G. Su, *J. Taiwan Inst. Chem. Eng.*, 42 (2011) 513.

3. T.Y. Wu, S.G. Su, K.F. Lin, Y.C. Lin, H.P. Wang, M.W. Lin, S.T. Gung, I.W. Sun, *Electrochim. Acta*, 56 (2011) 7278.
4. B. Baek, S. Lee, C. Jung, *Int. J. Electrochem. Sci.*, 6 (2011) 6220.
5. P.N. Tshibangu, S.N. Ndwandwe, E.D. Dikio, *Int. J. Electrochem. Sci.*, 6 (2011) 2201.
6. T.Y. Wu, S.G. Su, H.P. Wang, I.W. Sun, *Electrochem. Commun.*, 13 (2011) 237.
7. T.Y. Wu, S.G. Su, H.P. Wang, Y.C. Lin, S.T. Gung, M.W. Lin, I.W. Sun, *Electrochim. Acta*, 56 (2011) 3209.
8. I.W. Sun, Y.C. Lin, B.K. Chen, C.W. Kuo, C.C. Chen, S.G. Su, P.R. Chen, T.Y. Wu, *Int. J. Electrochem. Sci.*, 7 (2012) 7206.
9. T.Y. Wu, S.G. Su, S.T. Gung, M.W. Lin, Y.C. Lin, C.A. Lai, I.W. Sun, *Electrochim. Acta*, 55 (2010) 4475.
10. A.N. Soriano, A.M. Agapito, L.J.L.I. Lagumbay, A.R. Caparanga, M.H. Li, *J. Taiwan Inst. Chem. Eng.*, 42 (2011) 258.
11. T.Y. Wu, I.W. Sun, S.T. Gung, B.K. Chen, H.P. Wang, S.G. Su, *J. Taiwan Inst. Chem. Eng.*, 42 (2011) 874.
12. S. Ibrahim, M.R. Johan, *Int. J. Electrochem. Sci.*, 6 (2011) 5565.
13. T.Y. Wu, S.G. Su, Y.C. Lin, H.P. Wang, M.W. Lin, S.T. Gung, I.W. Sun, *Electrochim. Acta*, 56 (2010) 853.
14. H. Wang, L.X. Wu, Y.C. Lan, J.Q. Zhao, J.X. Lu, *Int. J. Electrochem. Sci.*, 6 (2011) 4218.
15. F.F. Liu, S.Q. Liu, Q.J. Feng, S.X. Zhuang, J.B. Zhang, P. Bu, *Int. J. Electrochem. Sci.*, 7 (2012) 4381.
16. H.A. Barham, S.A. Brahim, Y. Rozita, K.A. Mohamed, *Int. J. Electrochem. Sci.*, 6 (2011) 181.
17. S.K. Shukla, L.C. Murulana, E.E. Ebenso, *Int. J. Electrochem. Sci.*, 6 (2011) 4286.
18. N.V. Likhanova, O. Olivares-Xometl, D. Guzman-Lucero, M.A. Dominguez-Aguilar, N. Nava, M. Corrales-Luna, M.C. Mendoza, *Int. J. Electrochem. Sci.*, 6 (2011) 4514.
19. A. Zarrouk, M. Messali, H. Zarrok, R. Salghi, A.A. Ali, B. Hammouti, S.S. Al-Deyab, F. Bentiss, *Int. J. Electrochem. Sci.*, 7 (2012) 6998.
20. B.S. Ali, B.H. Ali, R. Yusoff, M.K. Aroua, *Int. J. Electrochem. Sci.*, 7 (2012) 3835.
21. M.H. Lin, Y.J. Liu, Z.H. Yang, Y.B. Huang, Z.H. Sun, Y. He, C.L. Ni, *Int. J. Electrochem. Sci.*, 7 (2012) 965.
22. C.H. Su, M.H. Chung, H.J. Hsieh, Y.K. Chang, J.C. Ding, H.M. Wu, *J. Taiwan Inst. Chem. Eng.*, 43 (2012) 573.
23. H. Shekaari, A. Kazempour, *J. Taiwan Inst. Chem. Eng.*, 43 (2012) 650.
24. Z.J. Wei, Y. Li, D. Thushara, Y.X. Liu, Q.L. Ren, *J. Taiwan Inst. Chem. Eng.*, 43 (2012) 363.
25. G.Q. Zhang, H.W. Yang, J.F. Gao, H.K. Zhang, C.B. Zheng, Y.L. Cao, Y.H. Wang, K.Q. Ding, *Int. J. Electrochem. Sci.*, 7 (2012) 7547.
26. P. Norouzi, M.R. Ganjali, F. Faridbod, S.J. Shahtaheri, H.A. Zamani, *Int. J. Electrochem. Sci.*, 7 (2012) 2633.
27. F. Faridbod, M.R. Ganjali, M. Hosseini, P. Norouzi, *Int. J. Electrochem. Sci.*, 7 (2012) 1927.
28. M.R. Ganjali, Z. Rafiei-Sarmazdeh, T. Poursaberi, S.J. Shahtaheri, P. Norouzi, *Int. J. Electrochem. Sci.*, 7 (2012) 1908.
29. A. Babaei, D.J. Garrett, A.J. Downard, *Int. J. Electrochem. Sci.*, 7 (2012) 3141.
30. M.R. Ganjali, T. Alizade, P. Norouzi, *Int. J. Electrochem. Sci.*, 7 (2012) 4800.
31. M.R. Ganjali, T. Alizade, B. Larijani, F. Faridbod, P. Norouzi, *Int. J. Electrochem. Sci.*, 7 (2012) 4756.
32. P. Norouzi, B. Larijani, M.R. Ganjali, *Int. J. Electrochem. Sci.*, 7 (2012) 7313.
33. T.Y. Wu, M.H. Tsao, S.G. Su, H.P. Wang, Y.C. Lin, F.L. Chen, C.W. Chang, I.W. Sun, *J. Braz. Chem. Soc.*, 22 (2011) 780.
34. M.H. Tsao, T.Y. Wu, H.P. Wang, I.W. Sun, S.G. Su, Y.C. Lin, C.W. Chang, *Mater. Lett.*, 65 (2011) 583.

35. S.Y. Ku, S.Y. Lu, *Int. J. Electrochem. Sci.*, 6 (2011) 5219.
36. T.Y. Wu, M.H. Tsao, F.L. Chen, S.G. Su, C.W. Chang, H.P. Wang, Y.C. Lin, I.W. Sun, *J. Iran. Chem. Soc.*, 7 (2010) 707.
37. I.W. Sun, H.P. Wang, H. Teng, S.G. Su, Y.C. Lin, C.W. Kuo, P.R. Chen, T.Y. Wu, *Int. J. Electrochem. Sci.*, 7 (2012) 9748.
38. T.Y. Wu, M.H. Tsao, F.L. Chen, S.G. Su, C.W. Chang, H.P. Wang, Y.C. Lin, W.C. Ou-Yang, I.W. Sun, *Int. J. Mol. Sci.*, 11 (2010) 329.
39. Y.X. An, P.J. Zuo, X.Q. Cheng, L.X. Liao, G.P. Yin, *Int. J. Electrochem. Sci.*, 6 (2011) 2398.
40. L.C. Xuan, Y.X. An, W. Fang, L.X. Liao, Y.L. Ma, Z.Y. Ren, G.P. Yin, *Int. J. Electrochem. Sci.*, 6 (2011) 6590.
41. H.M. Wang, S.Q. Liu, K. Huang, X.G. Yin, Y.N. Liu, S.J. Peng, *Int. J. Electrochem. Sci.*, 7 (2012) 1688.
42. H.M. Wang, S.Q. Liu, N.F. Wang, Y.N. Liu, *Int. J. Electrochem. Sci.*, 7 (2012) 7579.
43. H. Ganjali, M.R. Ganjali, T. Alizadeh, F. Faridbod, P. Norouzi, *Int. J. Electrochem. Sci.*, 6 (2011) 6085.
44. M.R. Ganjali, M.H. Eshraghi, S. Ghadimi, S.M. Moosavi, M. Hosseini, H. Haji-Hashemi, P. Norouzi, *Int. J. Electrochem. Sci.*, 6 (2011) 739.
45. M.R. Ganjali, T. Poursaberi, M. Khoobi, A. Shafiee, M. Adibi, M. Pirali-Hamedani, P. Norouzi, *Int. J. Electrochem. Sci.*, 6 (2011) 717.
46. P. Norouzi, M. Hosseini, M.R. Ganjali, M. Rezapour, M. Adibi, *Int. J. Electrochem. Sci.*, 6 (2011) 2012.
47. M.R. Ganjali, M.R. Moghaddam, M. Hosseini, P. Norouzi, *Int. J. Electrochem. Sci.*, 6 (2011) 1981.
48. M.R. Ganjali, M. Hosseini, M. Pirali-Hamedani, H.A. Zamani, *Int. J. Electrochem. Sci.*, 6 (2011) 2808.
49. M.R. Ganjali, M. Rezapour, S.K. Torkestani, H. Rashedi, P. Norouzi, *Int. J. Electrochem. Sci.*, 6 (2011) 2323.
50. P. Norouzi, M. Pirali-Hamedani, S.O. Ranaei-Siadat, M.R. Ganjali, *Int. J. Electrochem. Sci.*, 6 (2011) 3704.
51. F. Faridbod, H.A. Zamani, M. Hosseini, M. Pirali-Hamedani, M.R. Ganjali, P. Norouzi, *Int. J. Electrochem. Sci.*, 6 (2011) 3694.
52. M.R. Ganjali, S.O. Ranaei-Siadat, H. Rashedi, M. Rezapour, P. Norouzi, *Int. J. Electrochem. Sci.*, 6 (2011) 3684.
53. T.H. Tsai, K.C. Lin, S.M. Chen, *Int. J. Electrochem. Sci.*, 6 (2011) 2672.
54. M.R. Ganjali, T. Alizadeh, F. Azimi, B. Larjani, F. Faridbod, P. Norouzi, *Int. J. Electrochem. Sci.*, 6 (2011) 5200.
55. R. Mirshafian, M.R. Ganjali, P. Norouzi, *Int. J. Electrochem. Sci.*, 7 (2012) 1656.
56. J. Gao, J.G. Liu, W.M. Liu, B. Li, Y.C. Xin, Y. Yin, Z.G. Zou, *Int. J. Electrochem. Sci.*, 6 (2011) 6115.
57. T.Y. Wu, B.K. Chen, L. Hao, K.F. Lin, I.W. Sun, *J. Taiwan Inst. Chem. Eng.*, 42 (2011) 914.
58. T.Y. Wu, B.K. Chen, L. Hao, C.W. Kuo, I.W. Sun, *J. Taiwan Inst. Chem. Eng.*, 43 (2012) 313.
59. S.W. Peng, A.N. Soriano, R.B. Leron, M.H. Li, *J. Taiwan Inst. Chem. Eng.*, 42 (2011) 233.
60. T.Y. Wu, I.W. Sun, M.W. Lin, B.K. Chen, C.W. Kuo, H.P. Wang, Y.Y. Chen, S.G. Su, *J. Taiwan Inst. Chem. Eng.*, 43 (2012) 58.
61. T.Y. Wu, B.K. Chen, C.W. Kuo, L. Hao, Y.C. Peng, I.W. Sun, *J. Taiwan Inst. Chem. Eng.*, 43 (2012) 860.
62. A. Arce, H. Rodriguez, A. Soto, *Green Chem.*, 9 (2007) 247.
63. T.Y. Wu, H.C. Wang, S.G. Su, S.T. Gung, M.W. Lin, C.B. Lin, *J. Taiwan Inst. Chem. Eng.*, 41 (2010) 315.
64. X. Li, M. Hou, Z. Zhang, B. Han, G. Yang, X. Wang, L. Zou, *Green Chem.*, 10 (2008) 879.

65. J. Chen, S.K. Spear, J.G. Huddleston, R.D. Rogers, *Green Chem.*, 7 (2005) 64.
66. U. Domanska, M. Laskowska, *J. Solution Chem.*, 38 (2009) 779.
67. K. Tamura, M. Nakamura, S. Murakami, *J. Solution Chem.*, 26 (1997) 1199.
68. Z. Yu, H. Gao, H. Wang, L. Chen, *J. Chem. Eng. Data*, 56 (2011) 2877.
69. K.N. Marsh, J.A. Boxall, R. Lichtenthaler, *Fluid Phase Equilib.*, 219 (2004) 93.
70. T.Y. Wu, S.G. Su, S.T. Gung, M.W. Lin, Y.C. Lin, W.C. Ou-Yang, I.W. Sun, C.A. Lai, *J. Iran. Chem. Soc.*, 8 (2011) 149.
71. T.Y. Wu, L. Hao, C.W. Kuo, Y.C. Lin, S.G. Su, P.L. Kuo, I.W. Sun, *Int. J. Electrochem. Sci.*, 7 (2012) 2047.
72. T.Y. Wu, L. Hao, P.R. Chen, J.W. Liao, *Int. J. Electrochem. Sci.*, 8 (2013) 2606.
73. C.W. Kuo, C.W. Huang, B.K. Chen, W.B. Li, P.R. Chen, T.H. Ho, C.G. Tseng, T.Y. Wu, *Int. J. Electrochem. Sci.*, 8 (2013) 3834.
74. C.W. Kuo, W.B. Li, P.R. Chen, J.W. Liao, C.G. Tseng, T.Y. Wu, *Int. J. Electrochem. Sci.*, 8 (2013) 5007
75. T.Y. Wu, B.K. Chen, L. Hao, Y.C. Lin, H.P. Wang, C.W. Kuo, I.W. Sun, *Int. J. Mol. Sci.*, 12 (2011) 8750.
76. H. Rodriguez, J.F. Brennecke, *J. Chem. Eng. Data*, 51 (2006) 2145.
77. Y. Tian, X. Wang, J. Wang, *J. Chem. Eng. Data*, 53 (2008) 2056.
78. T.Y. Wu, H.C. Wang, S.G. Su, S.T. Gung, M.W. Lin, C.B. Lin, *J. Chin. Chem. Soc.*, 57 (2010) 44.
79. T.Y. Wu, B.K. Chen, L. Hao, Y.C. Peng, I.W. Sun, *Int. J. Mol. Sci.*, 12 (2011) 2598.
80. H. Eyring, M.S. John, Significant Liquid Structure, Wiley, New York, 1969.
81. H. Every, A.G. Bishop, M. Forsyth, D.R. MacFarlane, *Electrochim. Acta*, 45 (2000) 1279.
82. O. Redlich, A.T. Kister, *Ind. Eng. Chem.*, 40 (1948) 345.
83. A. Paul, P. Kumar, A. Samanta, *J. Phys. Chem. B*, 109 (2005) 9148.